

Supplement of Biogeosciences Discuss., 12, 17367–17392, 2015  
<http://www.biogeosciences-discuss.net/12/17367/2015/>  
doi:10.5194/bgd-12-17367-2015-supplement  
© Author(s) 2015. CC Attribution 3.0 License.



*Supplement of*

## **Temperature-mediated changes in microbial carbon use efficiency and $^{13}\text{C}$ discrimination**

**C. A. Lehmeier et al.**

*Correspondence to:* S. A. Billings ([sharon.billings@ku.edu](mailto:sharon.billings@ku.edu))

The copyright of individual parts of the supplement might differ from the CC-BY 3.0 licence.

1 **Supplementary Material**

2 **Exploring the principle of chemical and isotopic equilibrium in an open flow-through**  
3 **system at steady-state**

4 The basic idea of our approach is that the rate of CO<sub>2</sub> addition to the reactor headspace (Fig. 1)  
5 and the  $\delta^{13}\text{C}$  of this CO<sub>2</sub> represent the respiration rate of the microbial population and the  $\delta^{13}\text{C}$  of  
6 respired CO<sub>2</sub> at steady-state, respectively (Fig. 2). Steady-state here means that a bacterial  
7 population of constant size or density is growing at a constant rate, determined by the dilution  
8 rate of the reactor. The population then has a constant respiration rate, which is determined, in  
9 principle, by the specific environmental conditions at which the continuous flow reactor is  
10 operated.

11 The principle underlying this approach is based on established isotope theory, described in detail  
12 by Craig & Gordon (1965) and Fry (2006), and we are able to illustrate the validity of this  
13 principle with our experimental setup.

14 We had two gas cylinders, for which we directly measured concentration and  $\delta^{13}\text{C}$  of the CO<sub>2</sub>  
15 with the <sup>13</sup>CO<sub>2</sub>/<sup>12</sup>CO<sub>2</sub> analyzer via the flow path depicted in Supplementary Fig. 1. These  
16 measurements yielded that gas 1 had a CO<sub>2</sub> concentration of 302 ppm and a  $\delta^{13}\text{C}$  of -13.2 ‰ and  
17 gas 2 had a CO<sub>2</sub> concentration of 1015 ppm and a  $\delta^{13}\text{C}$  of -48.9 ‰.

18 We then installed the chemostat reactor into this flow path (Supplementary Fig. 2), in exactly the  
19 same way as in the experiments described in the main manuscript, just without the reservoir tank  
20 (compare with Fig. 1). We filled the reactor with approximately 1 liter of the same autoclaved

21 nutrient medium that we used in our experiments. The medium had a pH of 6.5, a temperature of  
22 22.1 °C and was not inoculated with microorganisms.

23 We first expelled inorganic C from the reactor medium, which will have been prevalent mainly in  
24 the form of  $\text{H}_2\text{CO}_3$  (aq) and  $\text{HCO}_3^-$  (Stumm and Morgan, 1981), by bubbling  $\text{CO}_2$ -free air  
25 through the medium for about 6 hours (Supplementary Fig. 3). As the  $\text{CO}_2$  concentration in the  
26 reactor headspace approached zero ppm, its apparent  $\delta^{13}\text{C}$  became more and more negative  
27 (Supplementary Fig. 3).

28 We then switched from  $\text{CO}_2$ -free air to gas 1, and let gas 1 bubble through the reactor medium  
29 for about 12 hours. Both concentration and  $\delta^{13}\text{C}$  in the reactor headspace changed rapidly after  
30 the switch and gradually approached 302 ppm and -13.2 ‰, the same as determined for gas 1 by  
31 direct measurements (Supplementary Fig. 3; and see above).

32 The gradual increase in headspace  $\text{CO}_2$  after switching from  $\text{CO}_2$ -free air to gas 1 reflects the  
33 build-up of  $\text{H}_2\text{CO}_3$  (aq) and  $\text{HCO}_3^-$  pools in the nutrient medium which are strong sinks for  $\text{CO}_2$ .  
34 However, when they reached their final sizes (dictated by temperature and pH of the nutrient  
35 medium), they had no further net sink capacity as evidenced by the invariant headspace  $\text{CO}_2$   
36 concentration identical to that of the gas 1 bottle measured directly (Supplementary Figs. 1, 3).

37 Thus, the system was in chemical equilibrium, which means that the  $\text{H}_2\text{CO}_3$  (aq) and  $\text{HCO}_3^-$  pool  
38 sizes did not change anymore. The re-establishment of a constant  $\delta^{13}\text{C}$  of reactor headspace  $\text{CO}_2$   
39 at the same value as obtained by direct measurement of the gas bottle proved that the system had  
40 also reached isotopic equilibrium, meaning that the  $\delta^{13}\text{C}$  of the export flux (measured reactor  
41 headspace  $\text{CO}_2$ ) was identical with the  $\delta^{13}\text{C}$  of the import flux  $\text{CO}_2$  (from the gas bottle;  
42 Supplementary Figs. 2, 3).

43 We then switched the gas supply from gas 1 to gas 2. Again, both concentration and  $\delta^{13}\text{C}$   
44 changed rapidly after the switch and gradually approached the values of the  $\text{CO}_2$  measured  
45 directly, i.e. 1015 ppm and a  $\delta^{13}\text{C}$  of -48.9 ‰ (Supplementary Fig. 3).

46 We then decreased the reactor temperature from 22.1 °C to 11.4 °C, a temperature range similar  
47 to that used in the experiments of the main manuscript. Both sizes and fractionation factors of  
48 the carbonate pool system must have reacted (Vogel et al., 1970; Mook et al., 1974; Stumm and  
49 Morgan, 1981; Szaran, 1997), and due to the slow and gradual change in reactor temperature,  
50 this translated into slow adjustments in reactor headspace  $\text{CO}_2$  concentration and  $\delta^{13}\text{C}$   
51 (Supplementary Fig. 3). However, twelve hours after initiation of the temperature change, the  
52 chemical and isotopic equilibria were re-established.

53 We then injected 2.5 mL of acetic acid ( $\text{C}_2\text{H}_4\text{O}_2$ ) into the nutrient medium which caused a  
54 change in pH from 6.5 to 3.45. Both concentration and  $\delta^{13}\text{C}$  of reactor headspace  $\text{CO}_2$  responded  
55 rapidly, as both sizes and fractionation factors of the carbonate pool system will have adjusted to  
56 the new pH. However, both concentration and  $\delta^{13}\text{C}$  of reactor headspace  $\text{CO}_2$  again returned to  
57 the values of the gas bottle within a few hours, again proving that a new steady-state of chemical  
58 and isotopic equilibrium was established.

59 At these three steady-states when bubbling gas 2, there will have been more or less pronounced  
60 differences in the sizes and the isotopic signatures of the inorganic C pools, caused by  
61 temperature and pH effects (Vogel et al., 1970; Mook et al., 1974; Stumm and Morgan, 1981;  
62 Szaran, 1997), but this did not change the fact that in this open flow-through system,  
63 concentration and  $\delta^{13}\text{C}$  of the import fluxes was the same as that of the export fluxes at steady-  
64 state.

65 In the chemostat experiments described in the main manuscript, we used this principle.  
66 Essentially, the only difference was that the source of CO<sub>2</sub> entering the reactor was not a gas  
67 bottle, but respiratory activity of a microbial population.

68 In our chemostat runs ranging from 13 °C to 26.5 °C, there will have been some differences in  
69 size and isotopic composition of the inorganic C pools, but they were irrelevant for the principle  
70 that what is going into the reactor is what is going out of the reactor, both in terms of respiration  
71 rate, as well as of  $\delta^{13}\text{C}$  of respired CO<sub>2</sub>.

72

73

74

75

76

77

78

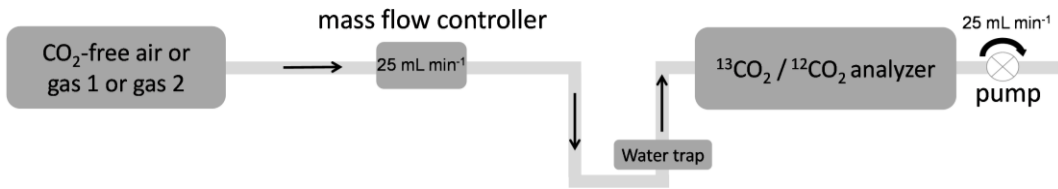
79

80

81

82

83 Supplementary Figure 1: Flow-path to measure gas from a cylinder with a  $^{13}\text{CO}_2/^{12}\text{CO}_2$  analyzer.  
84 See explanations in Supplementary Material and compare with Fig. 1 in the main manuscript.

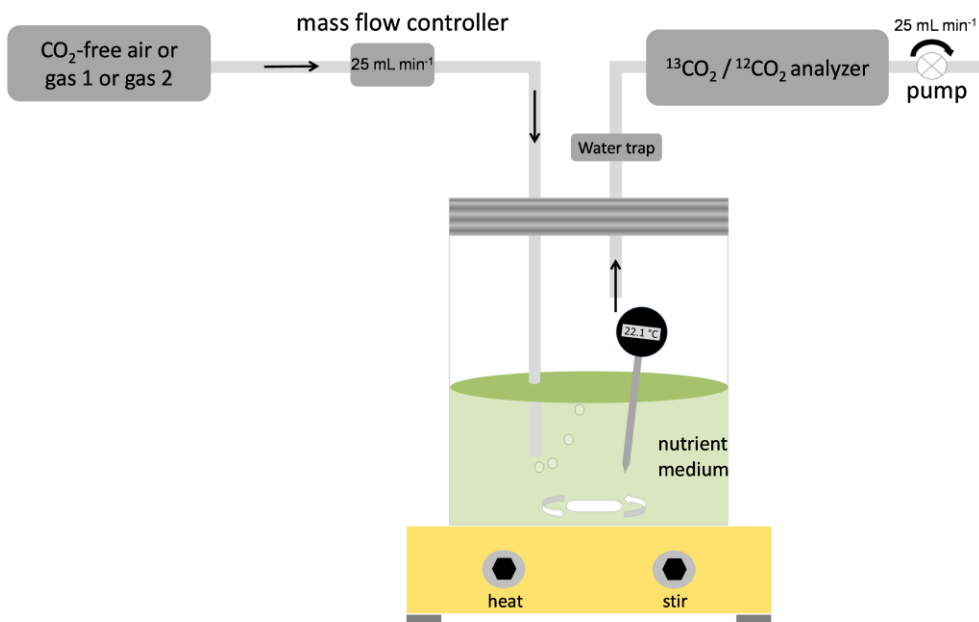


85

86

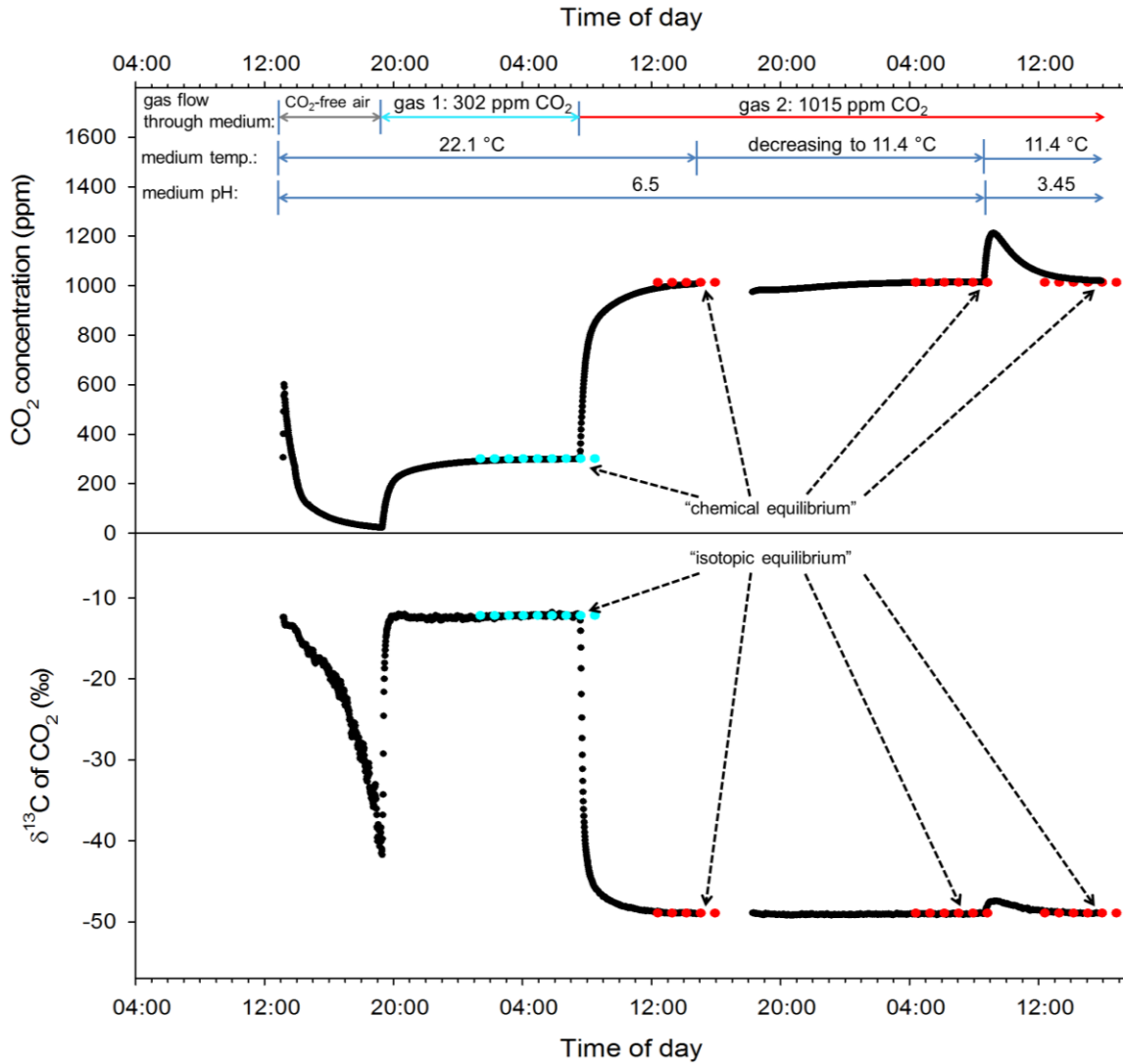
87

88 Supplementary Figure 2: Flow-path to measure cylinder gas bubbling through a sterile nutrient  
89 medium with a  $^{13}\text{CO}_2/^{12}\text{CO}_2$  analyzer. See explanations in the Supplementary Material and  
90 compare with Fig. 1 in the main manuscript.



91

92 Supplementary Figure 3: Time course of CO<sub>2</sub> concentration and δ<sup>13</sup>C measurements using the  
93 experimental system depicted in Supplementary Fig. 2. See Supplementary Material for a  
94 detailed description.



95

96

97

98

Supplementary Table 1. Process and growth parameters of independent continuous-culture chemostat runs with *P. fluorescens* at steady-state, performed at seven different temperatures of the reactor medium. Reactor biomass %C and %N and biomass C:N were obtained by elemental analysis of microbial dry matter, filtered from reactor medium with 0.2  $\mu\text{m}$  filters (n=4, but n=2 for 26.5 °C). Errors given are 1 SD.

reactor temperature (°C)	reactor volume (mL)	medium flow rate (mL h <sup>-1</sup> )	reactor half-life (h)	%C in biomass	%N in biomass	C:N ratio in biomass (w:w)
13	785	115.5	4.7	28.0 ± 1.1	7.9 ± 0.4	3.5
14.5	950	120	5.5	28.6 ± 0.3	7.6 ± 0.3	3.7
16	820	120	4.7	29.0 ± 0.6	8.4 ± 0.3	3.4
18	910	121	5.2	27.8 ± 0.9	7.7 ± 0.1	3.6
21	920	118	5.4	27.1 ± 0.5	7.9 ± 0.1	3.4
23.5	835	112	5.2	27.3 ± 0.2	6.9 ± 0.2	4.0
26.5	865	122	4.9	27.7 ± 0.1	7.8 ± 0.1	3.5